HHS Public Access

Author manuscript

Cell Rep. Author manuscript; available in PMC 2017 July 05.

Published in final edited form as:

Cell Rep. 2017 January 03; 18(1): 23–31. doi:10.1016/j.celrep.2016.12.024.

Biphasic Dependence of Glioma Survival and Cell Migration on CD44 Expression Level

Rebecca L. Klank[1,7], **Stacy A. Decker Grunke**[2,7], **Benjamin L. Bangasser**[1], **Colleen L. Forster**[3], **Matthew A. Price**[3], **Thomas J. Odde**[1], **Karen S. SantaCruz**[3], **Steven S. Rosenfeld**[4], **Peter Canoll**[5], **Eva A. Turley**[6], **James B. McCarthy**[3], **John R. Ohlfest**[2,8], and **David J. Odde**[1,9,*]

[1]Department of Biomedical Engineering, University of Minnesota, Minneapolis, MN 55455, USA

[2]Department of Pediatrics, University of Minnesota, Minneapolis, MN 55455, USA

[3]Department of Laboratory Medicine and Pathology, University of Minnesota, Minneapolis, MN 55455, USA

[4]Brain Tumor and Neuro-Oncology Center, Cleveland Clinic, Cleveland, OH 44195, USA

[5]Department of Pathology and Cell Biology, Columbia University Medical Center, New York, NY 10032, USA

[6]Department of Oncology, London Health Science Center, Schulich School of Medicine & Dentistry, Western University, London, Ontario N6A 4L6, Canada

SUMMARY

While several studies link the cell-surface marker CD44 to cancer progression, conflicting results show both positive and negative correlations with increased CD44 levels. Here, we demonstrate that the survival outcomes of genetically induced glioma-bearing mice and of high-grade human glioma patients are biphasically correlated with CD44 level, with the poorest outcomes occurring at intermediate levels. Furthermore, the high-CD44-expressing mesenchymal subtype exhibited a positive trend of survival with increased CD44 level. Mouse cell migration rates in ex vivo brain slice cultures were also biphasically associated with CD44 level, with maximal migration corresponding to minimal survival. Cell simulations suggest that cell-substrate adhesiveness is sufficient to explain this biphasic migration. More generally, these results highlight the potential

*Correspondence: oddex002@umn.edu.
[7]Co-first author
[8]Deceased contributor
[9]Lead Contact

SUPPLEMENTAL INFORMATION

Supplemental Information includes Supplemental Experimental Procedures, Supplemental Discussion, four figures, one table, and two movies and can be found with this article online at http://dx.doi.org/10.1016/j.celrep.2016.12.024.

AUTHOR CONTRIBUTIONS

S.A.D.G. designed the mouse tumor models, performed animal inoculations, and monitored animal survival/progression; R.L.K. conducted brain slice experiments, analyzed single-cell migration, and analyzed bioluminescence data; B.L.B. developed the 2D motor-clutch migration simulator; C.L.F., K.S.S., and P.C. conducted immunohistology of tumor sections; M.A.P. conducted and quantified the western blots; and T.J.O. analyzed the human survival data. S.S.R., E.A.T., J.B.M., J.R.O., and D.J.O. served as advisors to this work and provided significant intellectual contributions.

importance of non-monotonic relationships between survival and biomarkers associated with cancer progression.

In Brief

Klank et al. describe a biphasic relationship between CD44 expression levels and survival/cell migration rates in glioma. Intermediate CD44 levels in glioblastoma are linked to high tumor cell migration rates and poor survival, while both low and high CD44 levels were a positive prognostic indicator. These results illustrate the potential importance of non-monotonic relationships between survival and biomarkers associated with cancer progression.

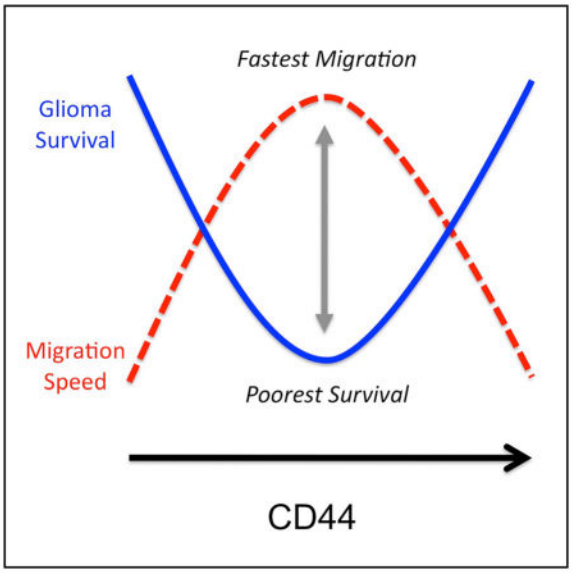

INTRODUCTION

At its most basic level, cancer progression is driven by aberrant cell proliferation and migration into previously healthy tissue. In the case of glioblastoma (grade IV glial brain cancer), even with standard treatment, median survival is approximately 15 months (Stupp et al., 2007) due to the invasiveness of the tumors (Hoelzinger et al., 2007; Lefranc et al., 2005). The brain is relatively rich in hyaluronic acid (HA), rather than collagen and fibronectin (Novak and Kaye, 2000), suggesting that CD44, a major transmembrane cell surface receptor for HA (Culty et al., 1990), could be an important mediator of glioma cell migration into the brain parenchyma (Breyer et al., 2000; Merzak et al., 1994). More generally, CD44 is reported to contribute to cancer invasion and has been implicated in epithelial-to-mesenchymal transition (Toole, 2009). However, while CD44 has been linked to multiple cancers, the literature is mixed on the importance of CD44 (Naor et al., 2002; Toole, 2009). In the case of glioma, some studies identified CD44 as a negative prognostic indicator of survival (Anido et al., 2010; Bhat et al., 2013; Jijiwa et al., 2011; Pietras et al., 2014), while others have found no correlation (Ranuncolo et al., 2002). Still others reported that, while CD44 concentration is positively correlated with glioma grade, within the highest malignancy grade, patients with expression above the median for that group experienced

longer survival than those below the median expression (Wei et al., 2010). At a mechanistic level, such apparently contradictory results are not surprising, due to the well-known biphasic dependence of cell migration on the strength of adhesion to the surrounding extracellular matrix (DiMilla et al., 1991, 1993; Palecek et al., 1997). More generally, biphasic relationships point toward optimality in the control of biological processes, such as the development of intestinal crypts (Itzkovitz et al., 2012) and the force transmission of filopodia (Chan and Odde, 2008). CD44 is a cell-adhesion molecule that extracellularly binds to HA and intracellularly is mechanically linked to the actin cytoskeleton through ezrin/radixin/moesin proteins (Ponta et al., 2003); therefore, cells would be expected to exhibit biphasic, not monotonic, migration behavior in response to increasing CD44 content. Since tumor dispersion can potentially contribute to overall tumor progression and mortality (Giese et al., 2003), we further hypothesized a biphasic relationship between CD44 expression level and survival. However, such relationships have not been established in vivo, and their relevance to cancer progression is unclear. Here, we report that human and mouse survival, as well as mouse cell migration in brain slices, are all biphasically dependent on CD44 level, consistent with predictions from a biophysical model for cell migration.

RESULTS

Survival in a Preclinical Model of Glioblastoma Has a Biphasic Dependence on CD44 Expression

To investigate the effects of CD44 on glioma progression, we used a de novo mouse glioma model that uses the Sleeping Beauty (SB) transposase system, which stably integrates oncogenic plasmid DNA into the host genome (Wiesner et al., 2009) and drives astrocytic tumors that are consistent with grade III and grade IV gliomas. Our SB-based model uses transforming plasmids encoding for constitutively active Nras (NrasG12V) and simian virus 40 large T antigen (SV40LgT) to mimic common human mutations frequently disrupted in human gliomas (e.g., RAS/PI3K, p53, RB). Altogether, four conditions were investigated (Figure 1A): CD44-positive wild-type (WT) animals (+/+), genetically matched CD44 knockout (KO) animals (−/−), KO animals with exogenous CD44 plasmid (KO+CD44), and WT animals with exogenous CD44 plasmid (WT+CD44) as models of CD44 overexpression. Western blotting of glioma cell lines derived from these models (two per condition) was used to confirm loss of CD44 and to determine the relative CD44 concentrations for each condition (Figure 1B). Quantification shows that injection of CD44 plasmid (KO+CD44 and WT+CD44) results in higher CD44 levels than WT, indicating that the addition of the CD44 plasmid generates an exogenous overexpression model, regardless of the mouse genotype. Therefore, the primary difference between the KO+CD44 and WT +CD44 conditions is the presence of endogenous levels of CD44 in the surrounding brain tissue cells in the latter case. Immunohistochemistry (IHC) analysis demonstrated that our mouse models are similar to human glioma (Figure 1C) and that CD44 was variably expressed by tumorigenic SV40LgT-expressing cells in our models (Figure 1D).

Survival was measured for each of the four conditions depicted in Figure 1A. As shown in Figure 2A, comparison of the Kaplan-Meier survival curves reveal that both KO mice and KO+CD44 mice exhibited a moderate yet significant survival increase compared to WT

animals (p = 0.0004 and p = 0.013, respectively, via log-rank test). The data presented in Figures 2A and 2B demonstrate that both KO and overexpression of CD44 improves survival (p = 0.001 for WT compared to WT+CD44 via log-rank test), a finding that would not be expected were survival to depend monotonically on CD44 levels. By plotting the median survival of each condition against the relative CD44 concentration, as shown in Figure 2B, our mouse model shows that survival is biphasic with respect to protein expression level of CD44 (as estimated via western blot in Figure 1B), with intermediate levels of CD44 exhibiting the worst outcome.

Survival of Patients with High-Grade Glioma Is Also Biphasic with CD44 Expression Level

We next investigated whether this biphasic relationship was present in the human disease. A recent study by Bhat et al. (2013) implicated CD44 as a negative prognosticator of survival in human glioblastoma patients. In their study, the authors compared the survival of newly diagnosed glioblastoma patients with high CD44 expression to that of patients with low CD44 expression, based on qualitative classification of stained histological sections. Using this high/low binning approach, they found a significant difference in the two survival curves, where higher CD44 expression correlated with worse survival outcomes. In our analysis, we utilized a slightly larger published dataset of human glioma survival from Phillips et al. (2006) that included quantifiable patient mRNA expression levels. Using categorical methods similar to those of Bhat et al., we pooled the data in two groups—one above the median CD44 expression level and one below—and found that the survival of the high-expressing group was statistically lower than that of the low-expressing group (p = 0.02; data not shown). We also took a continuum approach to the analysis of the data, which does not require an arbitrary threshold to assign groups, and we plotted survival times as a function of CD44 expression level (Figure 2C). The implication of the two-group (categorical) analysis is that more CD44 is worse for patient outcome; however, when we fit a line to the continuum data, we found that, while there is a slight negative slope (slope = −0.02, not shown), the 95% confidence interval of this parameter includes the value zero, meaning that the linear trend is not statistically significant (Figure 2D, left). Given the results from the mouse experiments, we then tested to determine whether a biphasic model corresponding to the survival in our mouse model (Figure 2B) would be more appropriate. We accomplished this by fitting to a quadratic, and this approach proved to be statistically significant (p = 0.015 for the quadratic term), indicating that patient outcomes actually improve once CD44 levels are sufficiently high (Figure 2C, black curve). The 95% confidence intervals for all coefficients in the quadratic fit do not include zero, meaning that all of the coefficients are statistically significant (Figure 2D, right). Moreover, it should be noted that we did not constrain our quadratic fit to a positive quadratic term, yet both animal and human data showed biphasic relationships that are concave-up, demonstrating that there is a minimum in survival in both cases at relatively intermediate CD44 levels. Independent of the statistical analysis, it is evident from direct examination of the data that there are very few long-term survivors at the intermediate CD44 level and that all of the long-term survivors (>200 weeks) either had low CD44 (<1,500) or high CD44 (>3,500). Censoring patients who were IDH1 mutant (Lai et al., 2011), which is closely associated with GCIMP (glioma-CpG island methylator phenotype)-positive status, removed seven patients but did not affect the biphasic trend (p = 0.20 for the linear model and p = 0.02 for the quadratic

model; see Supplemental Experimental Procedures). A similar analysis was completed using data available through The Cancer Genome Atlas (TCGA; Brennan et al., 2013). Although the numerical values of CD44 expression differ between the two datasets, the results from TCGA show a similar concave-up biphasic trend ($p = 0.025$; Figure S1A), while the linear trend was, again, not statistically significant ($p = 0.37$). Thus, we find that survival is biphasically dependent on CD44 level for both human glioma patients and genetically induced glioma-bearing mice, with the poorest prognosis in both cases at the intermediate CD44 level.

Human Glioma Subtypes Have Distinct Monophasic Trends with CD44 Expression

The original genome-wide transcriptomic analyses by Phillips et al. (2006) were seminal to the field in terms of establishing at least three glioma subtypes. Although more recent subtype classifications have emerged (Verhaak et al., 2010), subsequent classification analyses have confirmed the robustness and consistency of the proneural and mesenchymal subtypes in particular (Bhat et al., 2013). Therefore, we used the original Phillips classification scheme to determine whether our continuum approach to expression-level analyses would elucidate any subtype-specific trends. As shown in Figure 2C, we found that pro-neural subtypes tended to be lower in CD44 expression, proliferative subtypes were intermediate, and mesenchymal subtypes tended to have the highest CD44 expression. This is, perhaps, not surprising, as CD44 was used as a marker for the mesenchymal subtype (Phillips et al., 2006) and has been shown to positively correlate with a transition to a mesenchymal signature in glioma (Cheng et al., 2012).

Linear correlation analysis for survival as a function of CD44 within these three subtypes showed distinct monophasic trends based on Rab-14-normalized CD44 expression: (1) the proneural subtype demonstrated a modest negative linear correlation between survival and CD44 level ($p = 0.067$), (2) the proliferative subtype demonstrated no correlation ($p = 0.86$), and (3) the mesenchymal subtype demonstrated a strong positive correlation ($p = 0.00037$). The latter result is particularly interesting, because it implies that, while the mesenchymal subtype uses CD44 as a marker and exhibits overall poor survival outcome (Phillips et al., 2006), CD44 is actually a positive prognostic indicator within the mesenchymal subtype, with better survival observed at higher CD44 levels. In addition, it is worth noting that the three best fit linear correlations for the three subtypes (proneural, proliferative, and mesenchymal) all intersect at a point that nearly coincides with the quadratic fit to the overall data. This point, at a normalized CD44 level of 2,500, represents the worst case scenario for high-grade glioma outcome, where prognosis is poorest, a feature of the data that is evident even without statistical analysis. Overall, our analysis of the high-grade glioma subtypes is consistent with our analysis of the pooled continuum data, where low- and high-CD44 expressors have, on average, better survival outcomes and intermediate expressors have the worst average survival outcomes.

Net Proliferation Is Independent of CD44 Expression Level

Since CD44 has been linked to uncontrolled cell growth (Naor et al., 2002; Toole, 2009), we next examined the effects of CD44 on net tumor cell proliferation. BLI of the four conditions shows the relative progression of the tumors under different CD44 backgrounds

(Figure 3A). Integrated BLI signal at weeks 3 and 4 showed that initial tumor burden was greatest for KO animals (Figure 3B). More importantly, changes in integrated BLI signal between weeks 3 and 4 were not different between all cases ($p = 0.88$; Figure 3B, dashed lines). Growth rate calculations were not conducted after week 4 to avoid potential bias caused by substantial animal death (Figure 2A; Figure S2). To further assess net tumor cell proliferation, we also performed IHC staining of all four CD44 conditions for Ki67 and caspase-3 as indicators of proliferation and apoptosis, respectively. Staining for Ki67 and caspase-3 showed considerable variability in all four conditions and did not seem to correlate with survival or CD44 level (Figure 3C). Therefore, we conclude that inherent differences in net proliferation do not directly explain biphasic survival as a function of CD44 level. As others have found that antibody-mediated CD44 inhibition does not alter proliferation in vitro, but does affect migration (Yoshida et al., 2012), we instead focused on cell migration as an important driver of these cancers.

Simulated Whole-Cell Migration Is Biphasic with Increased Substrate Attachment

Cell migration is a dynamic physical process involving cell attachment to, and subsequent detachment from, the cell substratum (Lauffenburger and Horwitz, 1996). To test whether cell migration in a compliant environment predicts a biphasic migration rate, we developed a two-dimensional whole-cell model based on our “motor-clutch” stochastic model for cell protrusion and traction dynamics (Bangasser et al., 2013; Chan and Odde, 2008) (Figure S3; Table S1; Supplemental Experimental Procedures). Quantitative analyses of cell displacements (Figure 4A, upper row) allowed us to calculate the random-motility coefficient for each cell, a quantitative measure of dispersive capacity that is analogous to a diffusion coefficient (see Experimental Procedures) (Figure 4B). We found that maximal cell migration occurred when the clutch number was 250 (Movie S1), leading to a biphasic relationship between clutch number and motility. From these results, we predicted that changing CD44 concentration would predict a biphasic relationship between CD44 content and cell migration rates.

Cell Migration Is Biphasic with CD44 Expression Level and Anti-correlated to Animal Survival

To investigate the role of CD44 expression level on glioma cell migration in the mouse brains, we measured the motility of cells in ex vivo brain-slice cultures (Beadle et al., 2008). As shown in Figures 4C and 4D, WT cells exhibited the fastest migration overall and were found to exhibit statistically different migration than KO and WT+CD44 ($p < 0.001$ and $p = 0.03$, respectively). Although both KO+CD44 and WT+CD44 models exhibited similar motility, KO+CD44 was not found to be different from WT ($p = 0.17$), likely due to the presence of a higher percentage of faster moving KO+CD44 cells compared to WT+CD44 (Figure 4D, black boxes). However, when evaluated, instead, using a parametric one-way ANOVA, KO+CD44 was statistically different from WT ($p = 0.033$; see slopes on Figure 4C). Moreover, when both overexpression cases are pooled together, they are statistically different from WT using a Kruskal-Wallis test ($p < 0.02$; data not shown). KO animals displayed the least motility of all cases but were not found to be statistically different from the high-CD44-content WT+CD44 condition. Together, these ex vivo single-cell analyses demonstrate a biphasic relationship between CD44 protein expression and glioma cell

motility, where intermediate CD44 content (i.e., WT expression levels) leads to the greatest overall motility (Figure 4E, gray curve). These biphasic migration results are qualitatively consistent with simulation predictions (Figure 4B). Notably, biphasic migration outcomes are anti-correlated with biphasic survival outcomes, where maximal migration corresponds with minimal survival (Figure 4E, black curve), suggesting that CD44 may ultimately control survival by controlling cell migration and invasion in a non-monotonic manner.

DISCUSSION

In this study, we found that a simple high/low (monotonic) description of the role of CD44 in glioma progression masks important aspects of CD44 gene function; instead, a non-monotonic description reveals a previously unappreciated biphasic dependence of both survival and migration on CD44 expression level. Furthermore, we implicate CD44 as a potential molecular “clutch” in mediating migration and demonstrate that biphasic migration with respect to cell-substrate adhesiveness is sufficient to explain CD44’s role in glioma.

Implications for Bioinformatics, Biomarker Discovery, Genetic Analysis, and Therapeutic Strategy

Although CD44 inhibition was not tested in this study, this biphasic interpretation has important implications for clinical therapy. CD44 inhibition has been suggested by many as a therapeutic strategy for cancer (Breyer et al., 2000; Okada et al., 1996; Xu et al., 2010; Yoshida et al., 2012) and has recently been tested in clinical trials (Hoffman-LaRoche, n.d.); however, specifically in glioma but perhaps in other cancers as well, given the biphasic trend in survival, partial inhibition of CD44 in patients who are highly overexpressing could potentially drive tumors into a hyper-migratory state, thus promoting progression. Therefore, our results suggest a clinical strategy for glioma patient stratification based on CD44 expression level where patients are separated into high, intermediate, and low categories, rather than high and low categories as is typical in the literature. In this approach, intermediate-CD44-expressing patients (with an approximately normalized CD44 level between ~1,500 and ~3,500; Figure 2C) would be best suited for anti-CD44 therapy. By contrast, low-CD44-expressing patients would not expect to benefit, and high-CD44-expressing patients risk a worsened condition if only partial inhibition is achieved clinically.

EXPERIMENTAL PROCEDURES

Animals and Tumor Models

C57BL/6J ($CD44^{+/+}$, WT) and B6.129(Cg)-CD44tm1Hbg/J ($CD44^{-/-}$, KO) mice were purchased from Jackson Laboratory and used as described in the Supplemental Experimental Procedures. The mouse studies were performed under the oversight of the University of Minnesota IACUC.

Primary Cell Lines

Cell lines were established from the four mouse cohorts as described in the Supplemental Experimental Procedures.

Western Blotting

Cells were lysed and prepared for western blotting as described in the Supplemental Experimental Procedures.

Analysis of Published Human Data

CD44 expression data (Phillips et al., 2006) were analyzed as described in the Supplemental Experimental Procedures.

Bioluminescence

Animals were monitored for tumor progression using bioluminescence imaging (BLI) as described in the Supplemental Experimental Procedures.

Immunohistochemistry

Brain tumor sections were prepared for immunohistochemistry as described in the Supplemental Experimental Procedures.

Stochastic Whole-Cell Model

The stochastic whole-cell migration model was developed based on previously published motor-clutch models from our group (Bangasser and Odde, 2013; Bangasser et al., 2013; Chan and Odde, 2008). Our whole-cell model uses the Gillespie Stochastic Simulation Algorithm (Gillespie, 1977) to simulate an entire cell by connecting several motor-clutch modules together at a central cell body node and then balancing the forces at this node (Figure S3). Details are given in the Supplemental Experimental Procedures.

Single-Cell Migration Dynamics in Brain Slice Preparations

The four cohorts of mice were prepared for single-cell migration imaging using a modification of our previously described method (Beadle et al., 2008). Additional details are provided in the Supplemental Experimental Procedures.

Statistical Analysis

For mouse survival, log-rank statistical analyses were generated using GraphPad Prism software. Regression analyses for linear and quadratic fits of the human survival data were completed using R statistical software. Integrated bioluminescence intensity signals across conditions were analyzed by one-way ANOVA. For statistics on tumor growth rates, signal changes between weeks 3 and 4 were calculated for each animal, and the distributions of delta values were compared by one-way ANOVA. Distributions of cell random-motility coefficients for the different conditions were compared using a non-parametric, rank-based Kruskal-Wallis test with Bonferroni post hoc correction for multiple comparisons.

Supplementary Material

Refer to Web version on PubMed Central for supplementary material.

Acknowledgments

The study was supported by U.S. NIH grants RC1-CA145044 and R01-CA172986 to D.J.O. and S.R.R.; a University of Minnesota Institute for Engineering in Medicine Group grant to D.J.O.; U.S. NIH grant R01-CA138437; American Cancer Society grant RSG-09-189-01-LIB; the State of Minnesota, Minnesota Partnership for Biotechnology and Medical Genomics, and Children's Cancer Research Fund to J.R.O.; U.S. NIH grants T32-GM008471, T32-DA022616, and F31-NS67937 to S.A.D.; National Science Foundation Graduate Research Fellowship 00006595 to B.L.B.; and the Minnesota Supercomputing Institute.

References

Anido J, Sáez-Borderías A, Gonzàlez-Juncà A, Rodón L, Folch G, Carmona MA, Prieto-Sánchez RM, Barba I, Martínez-Sáez E, Prudkin L, et al. TGF-β receptor inhibitors target the CD44(high)/Id1(high) glioma-initiating cell population in human glioblastoma. Cancer Cell. 2010; 18:655–668. [PubMed: 21156287]

Bangasser BL, Odde DJ. Master equation-based analysis of a motor-clutch model for cell traction force. Cell Mol Bioeng. 2013; 6:449–459. [PubMed: 24465279]

Bangasser BL, Rosenfeld SS, Odde DJ. Determinants of maximal force transmission in a motor-clutch model of cell traction in a compliant microenvironment. Biophys J. 2013; 105:581–592. [PubMed: 23931306]

Beadle C, Assanah MC, Monzo P, Vallee R, Rosenfeld SS, Canoll P. The role of myosin II in glioma invasion of the brain. Mol Biol Cell. 2008; 19:3357–3368. [PubMed: 18495866]

Bhat KPL, Balasubramaniyan V, Vaillant B, Ezhilarasan R, Hummelink K, Hollingsworth F, Wani K, Heathcock L, James JD, Goodman LD, et al. Mesenchymal differentiation mediated by NF-κB promotes radiation resistance in glioblastoma. Cancer Cell. 2013; 24:331–346. [PubMed: 23993863]

Brennan CW, Verhaak RGW, McKenna A, Campos B, Noushmehr H, Salama SR, Zheng S, Chakravarty D, Sanborn JZ, Berman SH, et al. The somatic genomic landscape of glioblastoma. Cell. 2013; 155:462–477. [PubMed: 24120142]

Breyer R, Hussein S, Radu DL, Pütz KM, Gunia S, Hecker H, Samii M, Walter GF, Stan AC. Disruption of intracerebral progression of C6 rat glioblastoma by in vivo treatment with anti-CD44 monoclonal antibody. J Neurosurg. 2000; 92:140–149. [PubMed: 10616093]

Chan CE, Odde DJ. Traction dynamics of filopodia on compliant substrates. Science. 2008; 322:1687–1691. [PubMed: 19074349]

Cheng WY, Kandel JJ, Yamashiro DJ, Canoll P, Anastassiou D. A multi-cancer mesenchymal transition gene expression signature is associated with prolonged time to recurrence in glioblastoma. PLoS ONE. 2012; 7:e34705. [PubMed: 22493711]

Culty M, Miyake K, Kincade PW, Sikorski E, Butcher EC, Underhill C. The hyaluronate receptor is a member of the CD44 (H-CAM) family of cell surface glycoproteins. J Cell Biol. 1990; 111:2765–2774. [PubMed: 1703543]

DiMilla PA, Barbee K, Lauffenburger DA. Mathematical model for the effects of adhesion and mechanics on cell migration speed. Biophys J. 1991; 60:15–37. [PubMed: 1883934]

DiMilla PA, Stone JA, Quinn JA, Albelda SM, Lauffenburger DA. Maximal migration of human smooth muscle cells on fibronectin and type IV collagen occurs at an intermediate attachment strength. J Cell Biol. 1993; 122:729–737. [PubMed: 8335696]

Giese A, Bjerkvig R, Berens ME, Westphal M. Cost of migration: invasion of malignant gliomas and implications for treatment. J Clin Oncol. 2003; 21:1624–1636. [PubMed: 12697889]

Gillespie DT. Exact stochastic simulation of coupled chemical reactions. J Phys Chem. 1977; 81:2340–2361.

Hoelzinger DB, Demuth T, Berens ME. Autocrine factors that sustain glioma invasion and paracrine biology in the brain microenvironment. J Natl Cancer Inst. 2007; 99:1583–1593. [PubMed: 17971532]

Hoffman-LaRoche. Open-label multicenter 2-arm phase I study of RO5429083 with dose-escalation and extension cohorts, and imaging cohorts with RO5429083 and 89Zr-labeled RO5429083, in

patients with metastatic and/or locally advanced, CD44-expressing, malignant solid tumors. n.d. https://clinicaltrials.gov/ct2/show/NCT01358903

Itzkovitz S, Blat IC, Jacks T, Clevers H, van Oudenaarden A. Optimality in the development of intestinal crypts. Cell. 2012; 148:608–619. [PubMed: 22304925]

Jijiwa M, Demir H, Gupta S, Leung C, Joshi K, Orozco N, Huang T, Yildiz VO, Shibahara I, de Jesus JA, et al. CD44v6 regulates growth of brain tumor stem cells partially through the AKT-mediated pathway. PLoS ONE. 2011; 6:e24217. [PubMed: 21915300]

Lai A, Kharbanda S, Pope WB, Tran A, Solis OE, Peale F, Forrest WF, Pujara K, Carrillo JA, Pandita A, et al. Evidence for sequenced molecular evolution of IDH1 mutant glioblastoma from a distinct cell of origin. J Clin Oncol. 2011; 29:4482–4490. [PubMed: 22025148]

Lauffenburger DA, Horwitz AF. Cell migration: a physically integrated molecular process. Cell. 1996; 84:359–369. [PubMed: 8608589]

Lefranc F, Brotchi J, Kiss R. Possible future issues in the treatment of glioblastomas: special emphasis on cell migration and the resistance of migrating glioblastoma cells to apoptosis. J Clin Oncol. 2005; 23:2411–2422. [PubMed: 15800333]

Merzak A, Koocheckpour S, Pilkington GJ. CD44 mediates human glioma cell adhesion and invasion in vitro. Cancer Res. 1994; 54:3988–3992. [PubMed: 7518347]

Naor D, Nedvetzki S, Golan I, Melnik L, Faitelson Y. CD44 in cancer. Crit Rev Clin Lab Sci. 2002; 39:527–579. [PubMed: 12484499]

Novak U, Kaye AH. Extracellular matrix and the brain: components and function. J Clin Neurosci. 2000; 7:280–290. [PubMed: 10938601]

Okada H, Yoshida J, Sokabe M, Wakabayashi T, Hagiwara M. Suppression of CD44 expression decreases migration and invasion of human glioma cells. Int J Cancer. 1996; 66:255–260. [PubMed: 8603821]

Palecek SP, Loftus JC, Ginsberg MH, Lauffenburger DA, Horwitz AF. Integrin-ligand binding properties govern cell migration speed through cell-substratum adhesiveness. Nature. 1997; 385:537–540. [PubMed: 9020360]

Phillips HS, Kharbanda S, Chen R, Forrest WF, Soriano RH, Wu TD, Misra A, Nigro JM, Colman H, Soroceanu L, et al. Molecular subclasses of high-grade glioma predict prognosis, delineate a pattern of disease progression, and resemble stages in neurogenesis. Cancer Cell. 2006; 9:157–173. [PubMed: 16530701]

Pietras A, Katz AM, Ekström EJ, Wee B, Halliday JJ, Pitter KL, Werbeck JL, Amankulor NM, Huse JT, Holland EC. Osteopontin-CD44 signaling in the glioma perivascular niche enhances cancer stem cell phenotypes and promotes aggressive tumor growth. Cell Stem Cell. 2014; 14:357–369. [PubMed: 24607407]

Ponta H, Sherman L, Herrlich PA. CD44: from adhesion molecules to signalling regulators. Nat Rev Mol Cell Biol. 2003; 4:33–45. [PubMed: 12511867]

Ranuncolo SM, Ladeda V, Specterman S, Varela M, Lastiri J, Morandi A, Matos E, Bal de Kier Joffé E, Puricelli L, Pallotta MG. CD44 expression in human gliomas. J Surg Oncol. 2002; 79:30–35. [PubMed: 11754374]

Stupp R, Hegi ME, Gilbert MR, Chakravarti A. Chemoradiotherapy in malignant glioma: standard of care and future directions. J Clin Oncol. 2007; 25:4127–4136. [PubMed: 17827463]

Toole BP. Hyaluronan-CD44 interactions in cancer: paradoxes and possibilities. Clin Cancer Res. 2009; 15:7462–7468. [PubMed: 20008845]

Verhaak RGW, Hoadley KA, Purdom E, Wang V, Qi Y, Wilkerson MD, Miller CR, Ding L, Golub T, Mesirov JP, et al. Integrated genomic analysis identifies clinically relevant subtypes of glioblastoma characterized by abnormalities in PDGFRA, IDH1, EGFR, and NF1. Cancer Cell. 2010; 17:98–110. [PubMed: 20129251]

Wei KC, Huang CY, Chen PY, Feng LY, Wu TWE, Chen SM, Tsai HC, Lu YJ, Tsang NM, Tseng CK, et al. Evaluation of the prognostic value of CD44 in glioblastoma multiforme. Anticancer Res. 2010; 30:253–259. [PubMed: 20150644]

Wiesner SM, Decker SA, Larson JD, Ericson K, Forster C, Gallardo JL, Long C, Demorest ZL, Zamora EA, Low WC, et al. De novo induction of genetically engineered brain tumors in mice using plasmid DNA. Cancer Res. 2009; 69:431–439. [PubMed: 19147555]

Xu Y, Stamenkovic I, Yu Q. CD44 attenuates activation of the hippo signaling pathway and is a prime therapeutic target for glioblastoma. Cancer Res. 2010; 70:2455–2464. [PubMed: 20197461]

Yoshida T, Matsuda Y, Naito Z, Ishiwata T. CD44 in human glioma correlates with histopathological grade and cell migration. Pathol Int. 2012; 62:463–470. [PubMed: 22726066]

Highlights

- Glioblastoma survival in mice and humans depends biphasically on CD44 levels
- Intermediate CD44 levels are linked to high cell migration rates and poor survival
- High levels of CD44 correlate with better patient outcomes
- Net proliferation rates are independent of CD44, consistent with a biophysical theory

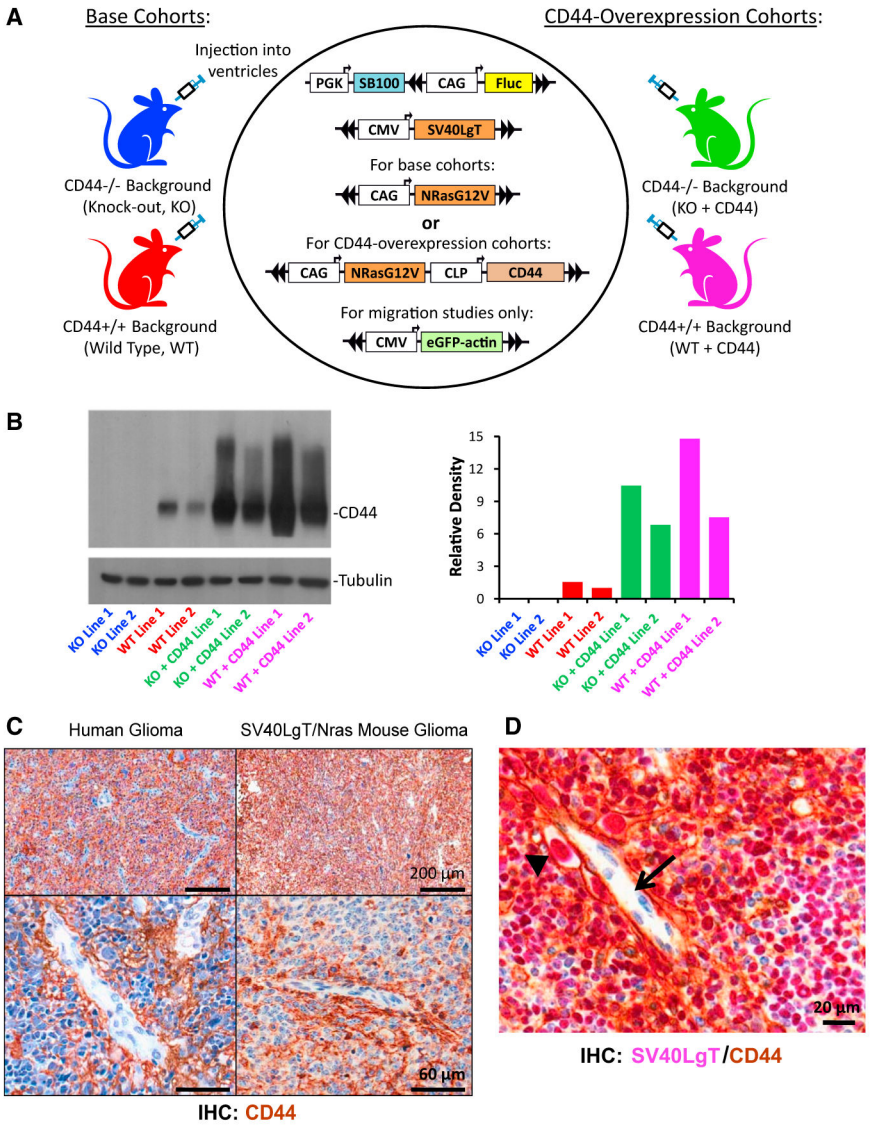

Figure 1. Control of CD44 Level in the Sleeping Beauty De Novo Mouse Glioma Model and Recapitulation of Human Glioma

(A) Schematic of mouse glioma models. Plasmids encoding for Sleeping Beauty transposase (SB100, light blue), oncogenes (orange), and Firefly Luciferase (yellow) were injected into CD44-competent (red) or matched CD44-deficient (blue) mice. Exogenous CD44 (pink) was included in KO+CD44 (green) and WT+CD44 (magenta) overexpression cohorts. For brain-slice migration studies, a fourth plasmid encoding EGFP-actin was included in each of the four conditions. Double arrows on the plasmids represent the SB100 binding sites.

(B) Left: western blot of CD44 expression for glioma cell lines derived from each of the four conditions (two per condition). Right: densitometry quantification of CD44 expression relative to WT line 2.

(C) Histological comparison of SV40LgT/Nras constructs in an WT mouse model to a human high-grade glioma shows similarities in CD44 staining. Top: low magnification shows homogeneous staining patterns in human and mouse tissues. Scale bars, 200 µm.

Bottom: higher magnification shows cell-to-cell variability and strong CD44 staining in the perivascular region. Scale bars, 60 μm.
(D) Two-color IHC for CD44 (brown, membrane) and SV40LgT (pink, nuclear) in WT mouse models confirms that CD44 expression is from SV40LgT-expressing glioma cells in the perivascular region (arrowhead). Arrow shows endothelial cells forming the vascular lumen.

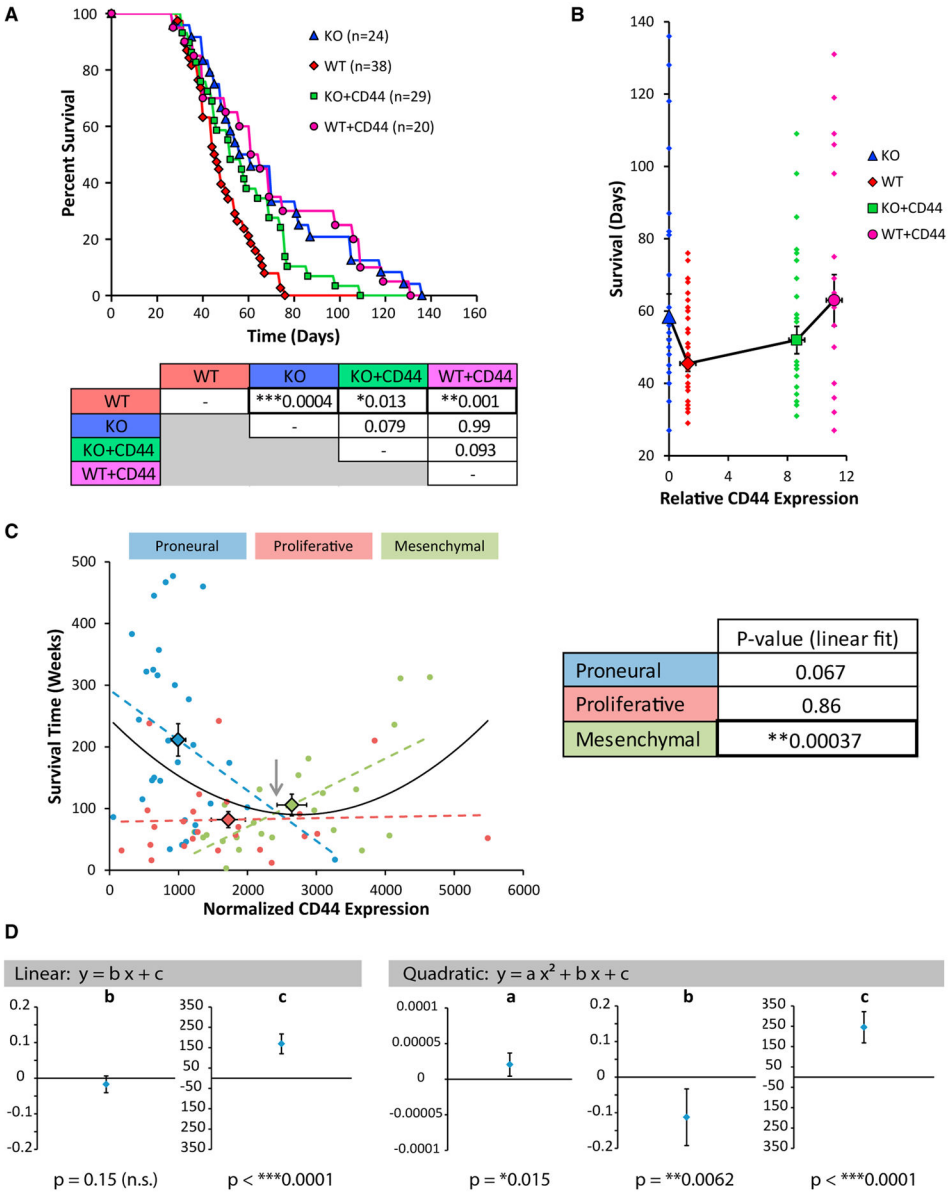

Figure 2. Mouse and Human Glioma Survival Are Biphasic with Respect to CD44 Expression Level

(A) Kaplan-Meier plot of animal survival for each of the four model conditions. The table below lists the p values for each pairwise comparison within an overall multiple comparisons statistical framework: *p < 0.05; **p < 0.01; ***p < 0.001.

(B) Biphasic dependence of survival on CD44 protein expression level, as measured in Figure 1B. Large colored markers indicate the median survival. Dots corresponding to each color indicate the survival times of individual animals. Horizontal error bars show the median ± coefficient of variation/√2. Vertical error bars correspond to ±SEM for survival.

(C) Biphasic dependence of human glioma patient survival on CD44 mRNA expression (Rab14 normalized) from data published in Phillips et al. (2006). Individual data points are color coded by subtype, as determined by Phillips et al. (2006). Quadratic fitting of all the

data (black curve) reveals a statistically significant non-monotonic/biphasic fit ($p = 0.015$) with upward concavity. A linear correlation analysis was conducted on each subtype separately to determine subtype-specific linear trends (right table). Notably, the mesenchymal subtype exhibited a strong positive linear correlation with CD44 level. Gray arrow indicates the point where the three linear fits approximately converge, closely coinciding with the minimum in the biphasic fit. Error bars correspond to ± SEM.
(D) Left: Values of each of the coefficients in the linear fit of all the human survival data are plotted with error bars indicating the 95% confidence intervals. While the data overall exhibit a slight downward linear trend, the slope is not statistically different from zero ($p = 0.15$). Right: values of each of the coefficients in the quadratic (biphasic) fit are plotted with error bars indicating the 95% confidence intervals. All coefficients in the quadratic fit are statistically significant, confirming a biphasic dependence of survival on CD44 level, with intermediate levels exhibiting the worst outcomes. n.s., not significant.

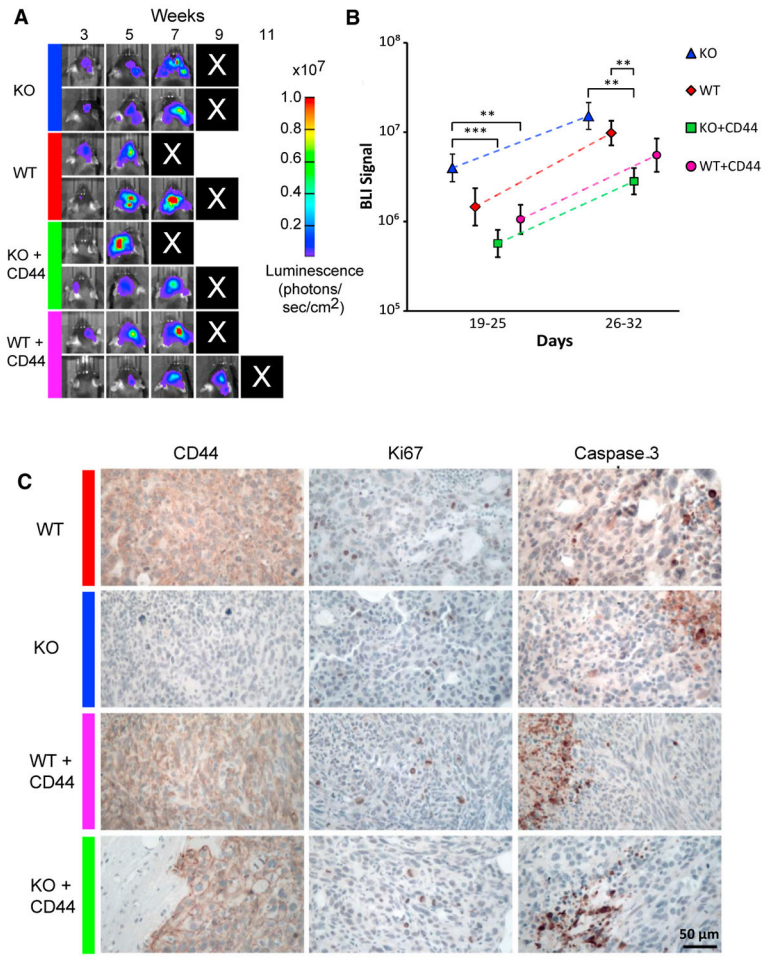

Figure 3. Net Proliferation Rate in the Mouse Gliomas Is Independent of CD44 Expression Level

(A) Bioluminescence imaging (BLI) of the four CD44 expression conditions showing glioma progression over time.

(B) Quantification of BLI integrated intensity. Mean integrated intensities at weeks 3 and 4 (days 19–25 and 26–32) are plotted ±SEM. At early time points, KO values are highest between all groups: **p < 0.01; ***p < 0.001. Slopes between weeks 3 and 4 (dashed lines) are not statistically different between all conditions (p = 0.88), indicating similar net growth rates.

(C) Immunohistology confirmed CD44 status and showed no discernable differences in Ki67 or caspase-3 staining across the four conditions. Left: CD44-positive cells are labeled in brown. Middle: brown indicates Ki67-positive (proliferating) cells for each of the conditions. Right: brown indicates caspase-3-positive (apoptotic) cells for each of the conditions. All slides are counter-stained with hematoxylin.

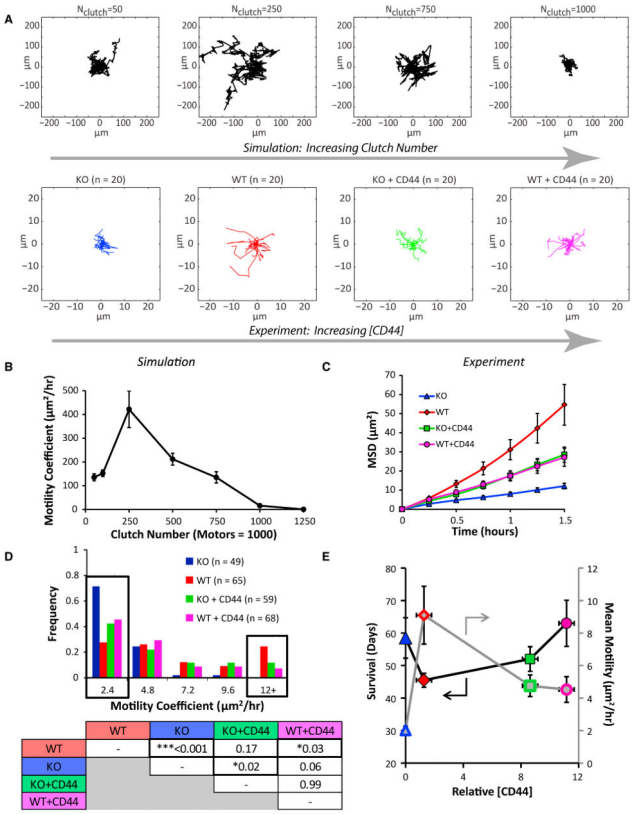

Figure 4. Single-Cell Motility in Biophysical Simulation and in Ex Vivo Brain Slices Is Biphasic with Respect to CD44 Expression Level

(A) Upper panels: wind rose plots of a representative subset of simulated motor-clutch model single-cell trajectories with increasing clutch number (representing CD44 level) over 10 hr of simulated time. Motor number is held constant at 1,000 per cell. Lower panels: wind rose plots of 20 randomly selected experimental cell trajectories for each animal condition over 1.5 hr.

(B) Simulation results demonstrating a biphasic, concave-down dependence of random-motility coefficient with respect to numbers of clutches (mean ± SEM).

(C) A mean squared displacement (MSD) as a function of time for each of the animal conditions. Error bars correspond to ± SEM.

(D) Histogram of random-motility coefficients for each tracked cell calculated from single-cell MSDs over 1.5 hr. The table below shows the pairwise comparisons of distributions for each condition using the non-parametric, rank-based Kruskal-Wallis test: *$p < 0.05$; **$p < 0.01$; ***$p < 0.001$, all with Bonferroni adjustment. Wild-type migration is statistically faster than both KO and WT+CD44, but not KO+CD44.

(E) Both animal survival (black, left axis) and cell motility (gray, right axis) are biphasic with respect to CD44 expression and anti-correlated with each other such that survival is poorest where migration is fastest. Horizontal error bars show the median ± coefficient of variation/√2. Vertical error bars correspond to ± SEM.